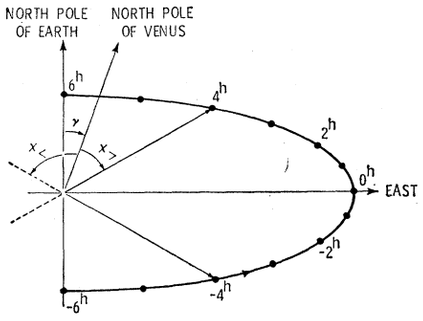

Fig. 1. Variation of the projected interferometer base line as the earth rotates during the day. When γ is small, the inclination angles $\chi_>$ and $\chi_<$, shown here for base lines at hour angles of $\pm$ 4h, are almost equal.

measured to be $(-3.6 \pm 5.0) \times 10^{-3}$, which implies a small polar heating with magnitude $\sim 2.0 \pm 2.8$ percent of the average surface temperature. In view of the experimental error the apparent heating is not statistically significant.

The total optical depth of the Venus atmosphere is large at 3.12 cm, being 1.8 for the model described by Gale *et al.* (*7*). The atmosphere thus both strongly emits radiation itself and attenuates the radiation from the surface. It is primarily the distribution of atmospheric absorptivity and temperature which is measured, and the surface temperature distribution is only important as it affects the atmospheric distribution. Thus we would place a limit of 3 percent on the polar cooling of the atmosphere seen at 3.12 cm. In view of the very sensitive temperature and pressure dependence of the absorptivities of the known constituents of Venus's atmosphere (*9*), the question of polar cooling of the surface must remain open.

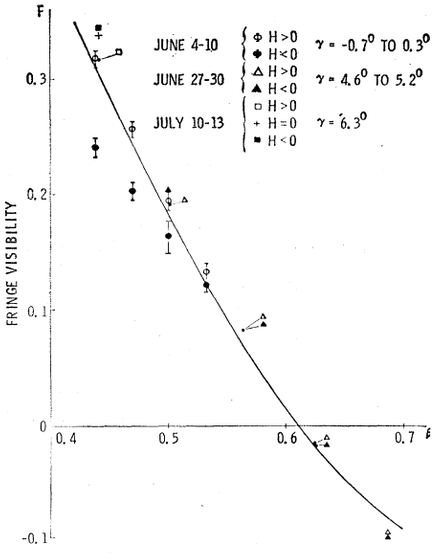

Fig. 2. Venus's fringe visibility $F(\beta)$ at 10.6 cm; β is the length of the base line, in wavelengths, multiplied by the planetary radius. The points show the observations, together with root-mean-square error bars for the data of 4 to 10 June 1964. The filled circles are believed to be in error. F for a uniform temperature planet is given by the solid curve.

A second technique for determining the polar cooling requires measurement of the integrated polarization of the radiation from the planet. The electromagnetic radiation from a given surface element of a planet will be partially linearly polarized (*10*). For a given polarization, maximum emission occurs at two points near the edge of the planet's disk, on the diameter defined by the polarization direction. If the planet is at a uniform temperature, these "Brewster angle" highlights will have a constant intensity for all choices of polarization direction, so that the integrated emission from the planet has no net polarization. With polar cooling, however, the highlights for polarization in the direction of the axis will be cooler than those for polarization in the direction of the equator. Thus, there will be a net polarization in the direction of the equator.

At 10.6-cm wavelength and for short interferometric base lines, so that the measurement was effectively that for a single telescope, Clark and Kuz'min (*1*) found the net polarization $p = 0.8 \pm 0.5$ percent at an angle $20° \pm 20°$ from the equator. For our atmospheric model, this implies a polar cooling of 23 ± 14 percent.

At 6-cm wavelength, Dickel (*11*) found $p = 0.5 \pm 0.9$ percent in the direction of the poles. The equatorially directed polarization expected on the basis of the model with 23 percent polar cooling is 0.3 percent, one-third of the stated error. It is apparent that the net polarization at 6 cm has not been detected.

It appears that present knowledge of the polar temperature of Venus's surface is very limited. While the 3.12-cm results have clearly shown that the poleward temperature variation of the atmosphere observed at this wavelength is small, only long wavelength radiation can penetrate the atmosphere, and measurements in this region are uncertain. However, it can be expected that interferometric measurements made during the 1969 inferior conjunction with the considerably improved accuracy now available, will determine the polar surface temperature within narrow limits.

W. A. Gale
A. C. E. Sinclair

Bellcomm, Inc.,
Washington, D.C. 20024

References and Notes

1. B. E. Clark and A. D. Kuz'min, *Astrophys. J.* **142**, 23 (1965).
2. W. F. Libby, *Science* **159**, 1097 (1968).
3. Percentage polar cooling is here defined as
$$100(T_{\text{equator}} - T_{\text{pole}})/T_{\text{average}}$$
where T is the absolute temperature.
4. G. L. Berge and E. W. Greisen, *Astrophys. J.*, in press.
5. J. D. Kraus, *Radio Astronomy* (McGraw-Hill, New York, 1966), chap. 6; A. T. Moffet, *Astrophys J.* **7**, Suppl., No. 67, 93 (1962).
6. I. I. Shapiro, *Science* **157**, 423 (1967).
7. W. Gale, M. Liwshitz, A. C. E. Sinclair, *ibid.*, **164**, 1059 (1969).
8. B. E. Clark, private communication.
9. W. Ho, I. A. Kaufman, P. Thaddeus, *J. Geophys. Res.* **71**, 5091 (1966).
10. C. E. Heiles and F. D. Drake, *Icarus* **2**, 281 (1963).
11. J. R. Dickel, *ibid.* **6**, 417 (1967).
12. We thank Drs. B. E. Clark and G. L. Berge for discussions.

17 February 1969; revised 3 June 1969

Red Sea Floor Origin: Rare-Earth Evidence

Abstract. *Abundance patterns of rare earths of submarine tholeiitic basalts from the axial trough of the Red Sea resemble those of basalts from mid-ocean ridges but are distinct from shield or plateau basalts of tholeiitic composition. These results imply that a similar magmatic process, related to spreading of sea floors, operates beneath the axial trough of the Red Sea and the crest of mid-ocean ridges.*

Seismic, gravity, magnetic, and heat-flow studies (*1*) of the Red Sea have led several workers to postulate that this area is a locus of ocean-floor spreading (*2, 3*). If this is true, the axial trough may be analogous to the central part of a mid-oceanic ridge, and the associated submarine basalts similar to those extruded on a mid-oceanic ridge.

To test this possibility, Chase (*4*) investigated the petrochemical characteristics of basaltic fragments raised in cores from the axial trough of the Red Sea between 19° and 23°N. These re-

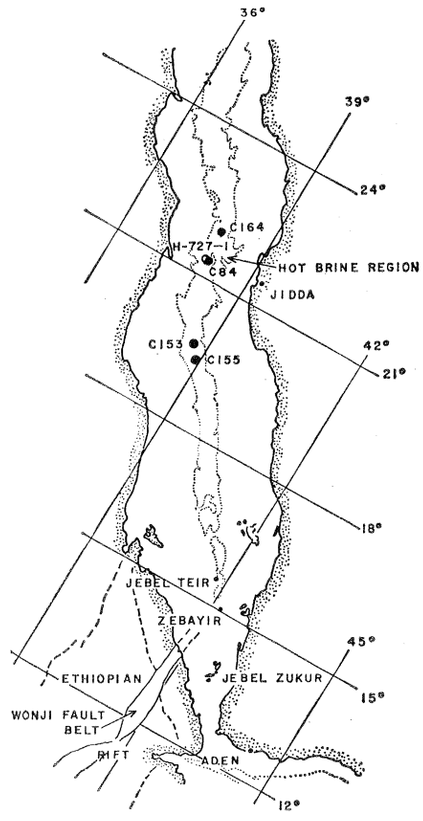

Fig. 1 (left). Locations of bottom samples containing volcanic material in the Red Sea. Dotted line is contour at 962 m (500 fathoms uncorrected) from Admiralty Chart C. 6359. Dashed lines delineate margins of Ethiopian rift and Wonji fault belt after P. A. Mohr. Numbers prefixed by C are *Chain* cruise 61 samples.

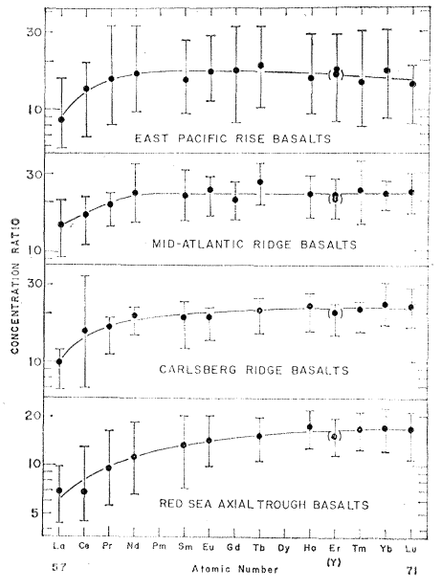

Fig. 2 (right). Average abundance of rare earths relative to chondrites of five submarine tholeiitic basals from the axial trough of the Red Sea; six submarine thoelittic basalts from the East Pacific Rise, data computed from (*9*) and (*10*); six submarine tholeiitic basalts from the Mid-Atlantic Ridge, data from (*9*); four submarine tholeiitic basalts from the Carlsberg Ridge in the northwest Indian Ocean, data from (*10*). Vertical bars represent extreme deviations of each element from the mean.

sults were, however, somewhat inconclusive. Although the Red Sea submarine basalts resemble oceanic basalts in their low potassium content and lack of normative nepheline, their total iron and phosphorus contents are high and are more typical of the alkaline basalts of the African rifts.

To further investigate possible geochemical similarities to typical mid-ocean ridge basalts, the rare earths ($_{57}$La to $_{71}$Lu, including $_{39}$Y) were determined in five of these basalt fragments by a neutron activation method (*5*).

Figure 1 shows the location of the basalts along the axial trough of the Red Sea. Table 1 lists the rare-earth contents of these tholeiitic basalts. Following the Masuda-Coryell practice (*6*), we compared the rare-earth abundance pattern of each rock, element by element, with a common reference, for example, the average of ordinary chondritic meteorites (*7*). The relative abundance of each rare earth (that is, enrichment factor relative to the reference) is plotted logarithmically versus a linear scale of the atomic numbers of the rare earths. These elements decrease in size with increasing atomic number, and an approximately linear relation exists between atomic number and reciprocal ionic radius (*8*).

Figure 2 is such a plot for the average of the five tholeiitic basalts from the axial trough of the Red Sea. The absolute level of the five individual patterns varies only within a small range, and the analytical errors vary from 4 to 10 percent depending on the element (*5*). Each of the five rocks has a rare-earth abundance trend similar to

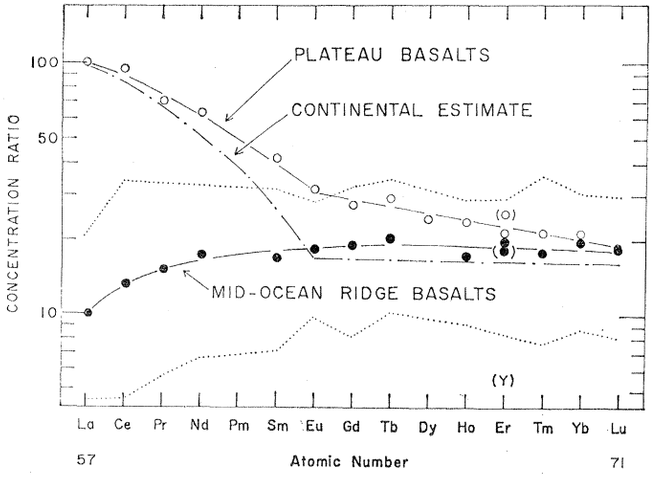

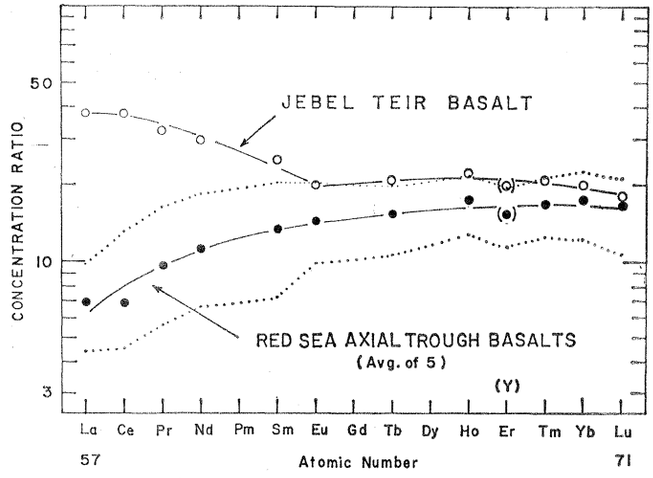

Fig. 3 (left). Average abundance of rare earths of tholeiitic basalts relative to chondrites for solid circles, mid-oceanic ridges (East Pacific Rise, Mid-Atlantic Ridge, Carlsberg Ridge, and Red Sea Axial Trough); the two dotted lines delineate the extreme deviations from this mean pattern; open circles, plateau basalts. Data for Columbia Plateau is from (*7*) and for Deccan from (*9, 11*); the dot-dashed line passes through an estimated rare-earth abundance average for the upper part of the continental crust (*10*). Fig. 4 (right). Abundance of rare earths relative to chondrites in one subaerial tholeiite from Jebel Teir Island, a shield volcano (open circles) is compared with the average abundance of rare earths of the five submarine tholeiitic basalts from the axial trough of the Red Sea (solid circles). Dotted lines delineate the extreme deviations from the mean.

Table 1. Rare-earth concentration (ppm) of five basaltic glass fragments collected in sediment cores along the axial trough of the Red Sea during the *Chain* cruise 61, and one subaerial tholeiitic basalt from Jebel Teir Island. Major element chemistry of the Red Sea basalts are available (*4*); for Jebel Teir basalt see (*19*).

Element	No. 84* 21° 21′N 28° 03.8′E	No. 153† 19° 43′N 38° 41′E	No. 155 19° 23.5′N 38° 54′E	No. 164 21° 59′N 37° 58.5′E	No. H-727-1 21° 24.4′N 38° 03.6′E	No. JT-1* Jebel Teir Island	Average of 20 chondrites (*7*)
La	1.89	1.15	2.61	2.96	1.90	11.26	0.30
Ce	7.54	3.82	4.58	11.0	5.50	31.5	0.84
Pr	1.11	0.669	1.21	1.96	1.13	3.86	0.12
Nd	7.01	3.77	8.05	10.8	5.74	17.3	0.58
Sm	2.61	1.68	2.90	4.25	2.71	5.19	0.21
Eu	1.04	0.699	1.14	1.49	0.949	1.47	0.074
Tb	0.727	0.524	0.871	0.974	0.753	1.02	0.049
Ho	0.946	0.732	1.22	1.25	0.930	1.26	0.057‡
Tm	0.388	0.338	0.536	0.501	0.391	0.521	0.025‡
Yb	2.71	2.44	3.82	3.74	2.44	3.42	0.17
Lu	0.495	0.433	0.598	0.656	0.414	0.562	0.031
Y	27.4	22.0	32.0	34.4	25.9	35.5	1.8
			Depth (meters)				
	1984	2703	2030	2282	1895		
			Core length (centimeters)				
	870	755	424	1178	0§		
			Depth of basalt in core (centimeters)				
	870		424	0	0		

* Partly crystalline. † Average of two analyses. ‡ Preferred values. § Fragments obtained during hydrographic lowering.

the average; on this basis the rocks form a uniform group. The abundance patterns show a progressive increase of the enrichment factor from the light rare earths (larger ions) toward the heavy rare earths (smaller ions), while the latter stay relatively constant. Thus, the larger the trivalent rare-earth ion, the greater is the depletion relative to the smaller rare-earth ions.

Such light rare-earth depleted patterns are characteristic of submarine tholeiites dredged from mid-oceanic ridges, as illustrated in Fig. 2 for the East Pacific Rise, Mid-Atlantic Ridge, and Carlsberg Ridge [northwest Indian Ocean (*9*)]. They are, however, quite distinct from rare-earth patterns of tholeiitic basalts produced by other types of vulcanicity and tectonic processes, as shown in Fig. 3, for instance, where tholeiites from the Columbia (*7*) and Deccan plateau-basalts (*9–11*) of continental areas have been compared with the rare-earth average pattern of submarine tholeiites of mid-oceanic ridges (including the Red Sea). Both tholeiitic plateau-basalts are light rare-earth enriched, as are most common rocks of the upper continental crust [for example, granitic rocks or detritic sediments (*12*)], whereas the submarine basalts are depleted in the light rare earths.

Further, in Fig. 4, the submarine tholeiitic basalts of the axial trough of the Red Sea are compared with a subaerial tholeiite from the Island of Jebel Teir, a shield volcano at the southern end of the Red Sea Trough (*13*). Again a noticeable difference is apparent mainly for the light rare earths, which are progressively enriched in the subaerial tholeiite. Similar differences were observed between tholeiites from oceanic ridges and geographically related seamounts or subaerial shield volcanoes of the Indian and East Pacific oceans (*10*). Progressive and systematic increases of the light rare earths with increasing alkalinity of lavas have been observed in several regions (*14*). However, what we are observing in Figs. 3 and 4 are chemical differences in tholeiite types which are clearly distinguished on rare-earth data but are not readily apparent in the major element chemistry of these basalts, the comparison here being limited to tholeiitic lavas only. Thus on the basis of rare-earth abundances and presumably other trace elements of similar behavior, there are tholeiites and tholeiites. Such differences are presumably related to tectonic processes, associated modes of vulcanicity, and the past chemical history of the source region (*15*) from which these lavas have derived (*10*).

It appears that the rare-earth patterns of the tholeiitic basalts of the axial trough of the Red Sea are similar to patterns found in submarine tholeiites from the crestal region of mid-oceanic ridges (*16*). The Red Sea basalts, except for sample 164, show a slightly more pronounced and progressive depletion of the rare earths, from the heavies to the lights, than tholeiitic basalts of mid-oceanic ridges. These small variations are, however, secondary effects not affecting our arguments, although they are admittedly important when one searches for the details of evolutionary mechanisms of sea floors (*10*). The pattern in these basalts is quite distinct from patterns of subaerial tholeiites of oceanic shield volcanoes or continental plateau basalts of tholeiitic composition. These data add further and unambiguously to the already existing geophysical evidence indicating that the axial trough of the Red Sea belongs to the worldwide oceanic rift system. It also indicates that the same magmatic process, related to spreading of the sea floor [that is, formation of new oceanic crust by magma self-healing the gaps produced apparently by divergent movements of rigid blocks of lithosphere (*2, 3, 17*)], must operate beneath the axial trough of the Red Sea and under the crest of mid-oceanic ridges. Such rare-earth results can significantly help to distinguish the various processes of vulcanism of the earth (*18*).

JEAN-GUY SCHILLING
Graduate School of Oceanography, University of Rhode Island, Kingston 02881

References and Notes

1. See for example, C. L. Drake and R. W. Girdler, *Geophys. J.* **8**, 473 (1964); S. T. Knott, E. T. Bunce, R. L. Chase, *Geol. Surv. Pap. Can.* **66-14**, 33 (196[illegible] J. G. Sclater, *Phil. Trans. Roy. Soc. London Ser. A Math. Phys. Sci.* **259**, 271 (1966); J. Woodside, C. O. Bowin, J. D. Phillips, in *Hot Brines and Recent Heavy Metal Deposits in the Red Sea: A Geochemical and Geophysical Account*, E. T. Degens and D. A. Ross, Eds. (Springer-Verlag, New York, in press), and references cited therein.
2. R. W. Girdler, *Geol. Surv. Pap. Can.* **66-14**, 65 (1966); F. J. Vine, *Science* **154**, 1405 (1966).
3. A. S. Laughton, *Geol. Surv. Pap. Can.* **66-14**, 78 (1966).
4. R. L. Chase, in *Hot Brines and Recent Heavy Metal Deposits in the Red Sea: A Geochemical and Geophysical Account*, E. T. Degens and D. A. Ross, Eds. (Springer-Verlag, New York, in press).
5. J-G. Schilling, thesis, Massachusetts Institute of Technology (1966).
6. A. Masuda, *J. Earth Sci. Nagoya Univ.* **10**, 173 (1962); C. D. Coryell, J. W. Chase, J. W. Winchester, *J. Geophys. Res.* **68**, 559 (1963).
7. R. A. Schmitt, R. H. Smith, D. A. Olehy, *Geochim. Cosmochim. Acta* **28**, 67 (1964).
8. This relation is best seen when precise radius determinations are used [D. H. Templeton and C. H. Dauben, *J. Amer. Chem. Soc.* **76**, 5327 (1954)].
9. Each individual pattern contained in the three averages has the same relative characteristics as the average, thus indicating again very uniform groups. Also, the absolute level of enrichment of these patterns varies only little despite the large distances separating the samples along the ridges and from ridge to ridge. Data for the Mid-Atlantic Ridge and part of the data for the East Pacific Rise are from F. A. Frey and L. Haskin, *J. Geophys. Res.* **69**, 775 (1964); F. A. Frey, M. D. Haskin, J. A. Poetz, L. A. Haskin, *ibid.* **73**, 6085 (1968); data for the Carlesberg Ridge and the rest of the data for the East Pacific Rise have been collected (*10*).
10. J-G. Schilling, "Sea floor evolution: evidence from rare-earth abundances," in preparation.
11. Y. A. Balashov and G. V. Nesterenko, *Geochem. Int.* **3**, 672 (1966).
12. L. A. Haskin, F. A. Frey, R. A. Schmitt, R. H. Smith, *Phys. Chem. Earth* **7**, 167 (1966).
13. The important problem of whether the volcanism of this island is related to the oceanic trough of the Red Sea or to the continental Ethiopian rift system was pointed out to me by I. G. Gass (personal communication). A preliminary account of the volcanism of the southern area of the Red Sea, where three major tectonic features join (Red Sea, Gulf of Aden, and African rift system) is given by I. G. Gass, D. I. J. Mallick, K. G. Cox, *Nature* **205**, 952 (1965); see also A. S. Laughton (*3*) for a description of this tectonically important triple junction, and P. A. Mohr, *Nature* **213**, 664 (1967).
14. J-G. Schilling and J. W. Winchester, *Science* **153**, 867 (1966); A. S. Pavlenko, Yu. A. Balashov, R. G. Gevorkyan, N. V. Turanskaya, V. I. Vernadskii, *Geokhimiya* **1966**, No. 2, 197 (1966); A. Masuda, *Earth Planet. Sci. Lett.* **4**, 284 (1968); A. G. Hermann, *Contrib. Mineral. Petrol.* **17**, 275 (1968).
15. Presumably the mantle for the submarine tholeiites erupted along mid-ocean ridges, but not necessarily for tholeiites of plateau type. The possibility remains that these plateau basalts were (i) affected by crustal contamination of melts ascending from the mantle or, (ii) produced by melting of the lower part of the continental crust.
16. In Table 1, sample 155 shows an anomalously low value for cerium. We have observed, inconsistently, either anomalously high or low Ce values in other submarine basalts from the Indian Ocean or East Pacific Rise, but not in subaerial basalts. Trivalent Ce can easily be oxidized to the tetravalent state, producing an anomalous behavior of Ce relative to other rare earths; for example, manganese nodules are enriched in Ce, whereas seawater is impoverished [A. M. Ehrlich, thesis, Massachusetts Institute of Technology, (1968)]. The Ce anomalies in basalts confined to submarine eruptions may thus possibly be attributed to secondary, posteruptional processes such as those due to seawater alteration, growth of Mn crusts on the surface of submarine basalts, or formation of Mn nodules. However, these Ce variations may simply be due to analytical errors, since the determination of this element presents greater analytical uncertainties than that of adjacent rare earths.
17. D. P. McKenzie and R. L. Parker, *Nature* **216**, 1276 (1967); W. J. Morgan, *J. Geophys. Res.* **73**, 1959 (1968); X. LePichon, *ibid.*, p. 3661; B. Isacks, J. Oliver, L. R. Sykes, *ibid.*, p. 5855.
18. J-G. Schilling and J. W. Winchester, in *Mantles of the Earth and Terrestrial Planets*, S. K. Runcorn, Ed. (Interscience, London, 1967), p. 267.
19. I. G. Gass, in preparation.

20. I am indebted to R. L. Chase, D. A. Ross, C. L. Drake, and I. G. Gass for furnishing the samples analyzed; A. F. DiMeglio, M. P. Doyle, and their crew of the Rhode Island Nuclear Science Center for the neutron irradiations and for laboratory facilities; J. L. Stevens, Mrs. H. H. Myers, R. W. Cooke, and Mrs. E. J. Sekator for carrying out parts of the rare-earth analyses; and R. L. Chase, P. A. Mohr, J. de Boer, D. Hermes, and J. W. Winchester for reading the manuscript and for suggestions. Supported by Office of Naval Research [Nonr 396(08)].

25 April 1969

Sunglint Patterns: Unusual Dark Patches

Abstract. *Anomalous dark areas in sunglint patterns are occasionally seen in photographs taken by the Applications Technology Satellite. These dark areas appear to be caused by relatively calm surface conditions against a background of higher sea states. Evidence of cold water temperatures suggest the presence of upwelling. These sightings may thus be of importance to the fishing industry.*

With the initiation of the geosynchronous Applications Technology Satellite (ATS) series in December 1966, continuous monitoring of specific geographic areas first became possible. From their orbiting height of approximately 36,000 km, these satellites maintain a fixed position in space relative to the earth. As such, it is possible to develop time-sequence pictures showing diurnal changes in various features at the earth's surface.

During a study of these full-disk, ATS picture sequences, a number of irregularities in the overall sunglint patterns were noted (*1*). In the course of a day, the sunglint may be observed to move from east to west across the face of the earth at a latitude intermediate between that of the satellite and the sun. Isolated areas appeared within the sunglint pattern which were alternately dark, bright, and then dark again relative to their background as

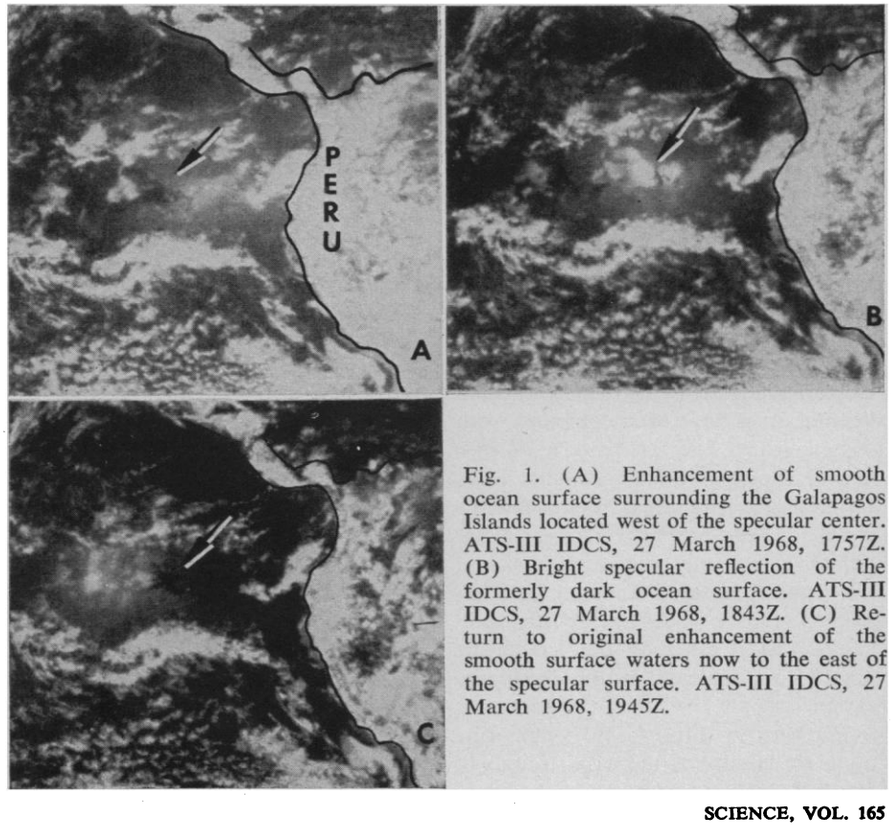

Fig. 1. (A) Enhancement of smooth ocean surface surrounding the Galapagos Islands located west of the specular center. ATS-III IDCS, 27 March 1968, 1757Z. (B) Bright specular reflection of the formerly dark ocean surface. ATS-III IDCS, 27 March 1968, 1843Z. (C) Return to original enhancement of the smooth surface waters now to the east of the specular surface. ATS-III IDCS, 27 March 1968, 1945Z.